Article

# Engineering Cyclohexanone Monooxygenase for the Production of Methyl Propanoate

Hugo L. van Beek, Elvira Romero, and Marco W. Fraaije

*ACS Chem. Biol.*, **Just Accepted Manuscript** • DOI: 10.1021/acschembio.6b00965 • Publication Date (Web): 09 Dec 2016



ACS Chemical Biology is published by the American Chemical Society. 1155 Sixteenth Street N.W., Washington, DC 20036

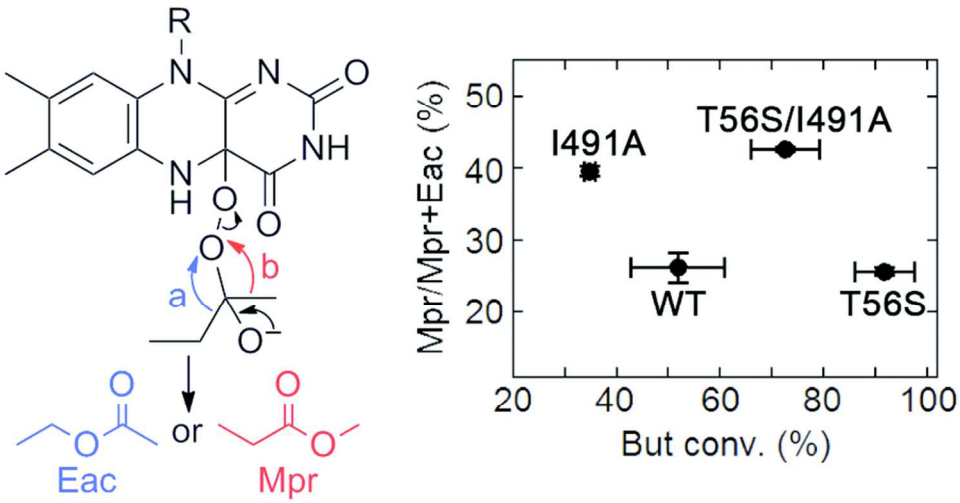


TOC figure

80x39mm (300 x 300 DPI)

# Engineering Cyclohexanone Monooxygenase for the Production of Methyl Propanoate

Hugo L. van Beek,[δ,ϕ,§] Elvira Romero,[δ,§] and Marco W. Fraaije[δ,*]

[δ]Molecular Enzymology Group, University of Groningen, Nijenborgh 4, 9747AG Groningen, The Netherlands

**ABSTRACT:** A previous study showed that cyclohexanone monooxygenase from *Acinetobacter calcoaceticus* (AcCHMO) catalyzes the Baeyer-Villiger oxidation of 2-butanone, yielding ethyl acetate and methyl propanoate as products. Methyl propanoate is of industrial interest as a precursor of acrylic plastic. Here, various residues near the substrate and $NADP^+$ binding sites in AcCHMO were subjected to saturation mutagenesis to enhance both the activity on 2-butanone and the regioselectivity toward methyl propanoate. The resulting libraries were screened using whole cell biotransformations, and headspace gas chromatography-mass spectrometry was used to identify improved AcCHMO variants. This revealed that the I491A AcCHMO mutant exhibits a significant improvement over the wild type enzyme in the desired regioselectivity using 2-butanone as a substrate (40% *vs.* 26% methyl propanoate, respectively). Another interesting mutant is the T56S AcCHMO mutant, which exhibits a higher conversion yield (92%) and $k_{cat}$ (0.5 $s^{-1}$) than wild type AcCHMO (52% and 0.3 $s^{-1}$, respectively). Interestingly, the uncoupling rate for the T56S AcCHMO mutant is also significantly lower than that for the wild type enzyme. The T56S/I491A double mutant combined the beneficial effects of both mutations leading to higher conversion and improved regioselectivity. This study shows that even for a relatively small aliphatic substrate (2-butanone), catalytic efficiency and regioselectivity can be tuned by structure-inspired enzyme engineering.

Baeyer-Villiger monooxygenases (BVMOs) are flavin-dependent enzymes that catalyze the insertion of an oxygen atom next to the carbonyl group of ketone substrates, producing esters or lactones.[1] Oxidation of aldehydes, heteroatoms, and epoxidations can also be carried out by BVMOs.[1] These reactions are of remarkable industrial interest, for example in the synthesis of valuable steroids, sulfoxides, *β*-amino acids, and ene- and enol-lactones.[2,3] BVMOs generally exhibit high regio- and stereoselectivity in contrast to the chemical oxidants utilized for Baeyer-Villiger reactions such as peracids or hydrogen peroxide.[1] Implementing BVMOs instead of these chemicals also avoids several environmental and safety issues.

The overall catalytic cycle of BVMOs with ketone substrates is well understood, based on steady-state and rapid kinetic studies (Scheme 1).[4-6] After binding of NADPH to the enzyme, the 4(*R*)-hydride is transferred from NADPH to the FAD N5 atom. The reduced FAD reacts with dioxygen to form a C4a-peroxyflavin intermediate. In the absence of a ketone substrate, the C4a-peroxyflavin intermediate decays yielding hydrogen peroxide, $NADP^+$, and oxidized FAD. This process is known as uncoupling. Alternatively, the C4a-peroxyflavin intermediate carries out a nucleophilic attack on the carbonyl carbon of the substrate resulting in the formation of a tetrahedral Criegee intermediate. The rearrangement of the Criegee intermediate results in the formation of C4a-hydroxyflavin and an ester or lactone. After elimination of a water molecule from the C4a-hydroxyflavin, the FAD is returned to the oxidized state. The ester or lactone and $NADP^+$ are released from the enzyme active site to close the catalytic cycle. Certain BVMO-catalyzed reactions yield either two regioisomeric products or only the unexpected one, broadening the applicability of these enzymes in organic synthesis.[1] Electronic and steric effects control the regioselectivity of these reactions. After forming the Criegee intermediate, one of the carbon atoms adjacent to the substrate carbonyl group migrates to the closest oxygen atom of the peroxide group (**Scheme 1, 3A**). The antiperiplanar conformation of the migrating carbon-carbon bond and the oxygen-oxygen bond allows the migration to proceed.[7,8] The normal regioisomer is formed by the migration of the more nucleophilic carbon, which in most cases is the more substituted carbon. A different product, the abnormal regioisomer, is formed when the less nucleophilic carbon migrates during the Criegee rearrangement. Formation of the abnormal regioisomer has been detected in the reaction of BVMOs with benzo-fused ketones,[9] cycloalkanones,[3,10,11] cycloalkenones,[3] linear aliphatic *β*-hydroxyketones,[12] *β*-aminoketones,[13] and long ketones (8-12 carbons).[14]

Recently, we reported that several cyclohexanone monooxygenases (CHMO; EC 1.14.13.22) catalyze the Baeyer-Villiger oxidation of 2-butanone, yielding the normal product ethyl acetate and a significant amount of the abnormal product methyl propanoate (14–27% of total product).[15] All CHMOs capable of carrying out this reaction exhibited considerably lower activity on 2-butanone than on cyclohexanone.[15] In the present work, we aim to increase the activity of a CHMO on 2-butanone and to shift the regioselectivity of this reaction to favor the formation of methyl propanoate. Methyl propanoate is of industrial interest because it can be converted into methyl methacrylate by reaction with formaldehyde.[16] Methyl methacrylate is polymerized to form the acrylic plastic poly(methyl methacrylate), which is used in many applications. A

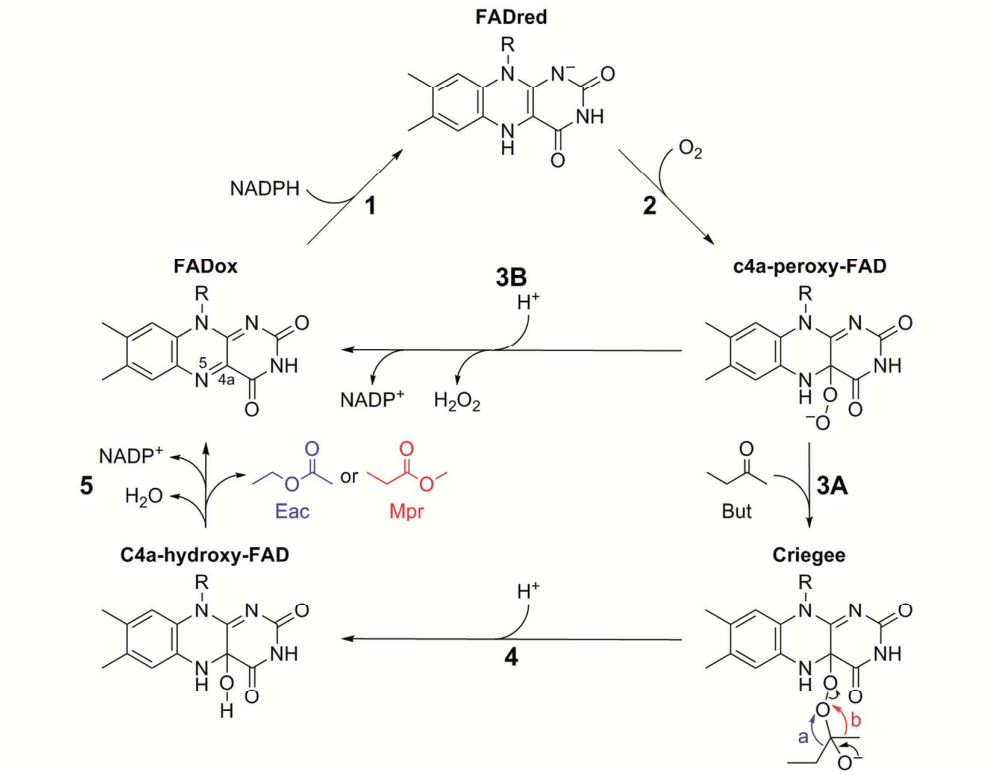


**Scheme 1.** Catalytic cycle of AcCHMO with 2-butanone as a substrate. For FAD, R is ribitol adenosine diphosphate. Either ethyl acetate (Eac) or methyl propanoate (Mpr) is produced.

renewable feedstock may be used to produce 2-butanone.[17,18] In addition, methyl propanoate is used for flavoring and as a solvent.[19,20]

Recently, a complete reversal in the regioselectivity of the reaction of CHMO with (+)-*trans*-dihydrocarvone has been achieved by replacing only three active site residues.[11] Another study showed that the reaction of a single mutant of cyclopentanone monooxygenase (CPMO; 1.14.13.16) with 3-(2-oxocyclohexyl)propanenitrile preferentially produced the abnormal regioisomer in contrast to the wild type (WT) enzyme.[10] Both works indicate that steric effects can control the regioselectivity of a reaction by influencing the exact position of the substrate in the active site. Although we anticipated that controlling the regioselectivity may be more difficult when smaller substrates are used, we engineered the CHMO from *Acinetobacter calcoaceticus* NCIMB 9871 (AcCHMO) to increase the ratio of the desired abnormal product over the normal product in the reaction with 2-butanone. AcCHMO was selected for this work because it shows better or similar activity and regioselectivity toward methyl propanoate than other CHMOs.[15] Since there is no available crystal structure of AcCHMO, a homology model of AcCHMO,[21] available BVMO crystal structures, and data from previous mutagenesis studies were used to select 35 residues as targets for site-saturation mutagenesis. The resulting libraries were screened in 96-well plates using headspace gas chromatography-mass spectrometry (GC-MS). Several improved variants were discovered and characterized using steady-state and rapid kinetics to elucidate the specific reaction steps affected by the mutations.

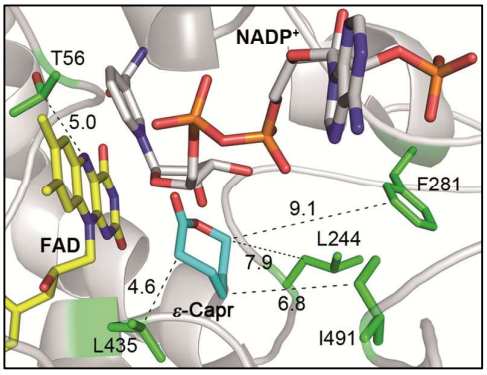


**Figure 1.** Active site of WT AcCHMO. A selection of residues that were targeted in this study is highlighted in sticks (green carbons). A superimposition of the WT AcCHMO model and the crystal structure of RhCHMO in complex with ε-caprolactone (ε-Capr) was carried out to infer the position of the ligand (cyan carbons). Distances in

Å between residues and either the ligand or FAD (yellow carbons) are indicated above the broken lines.

## RESULTS AND DISCUSSION

**Design of the Libraries.** Our previous study showed that AcCHMO catalyzes the Baeyer-Villiger oxidation of 2-butanone yielding both ethyl acetate and methyl propanoate (**Scheme 1**).[15] Here, we have carried out saturation mutagenesis to increase the activity of AcCHMO on 2-butanone and to improve the regioselectivity toward methyl propanoate. Three libraries were generated named A, B, and C (**Table S1**) and, in total, 35 residues were targeted for randomization. The randomization sites were chosen using a homology model of AcCHMO that was constructed for a previous study.[21] We superimposed this model onto the crystal structure of phenylacetone monooxygenase (PAMO; EC 1.14.13.92) in complex with the inhibitor MES and $NADP^+$ (PDB ID: 2YLT; RMSD = 1.06).[22] This task allowed inferring the position of the above ligands relative to that of the residues in the AcCHMO model. Various AcCHMO residues near the substrate and $NADP^+$ binding sites (≤ 15 Å) were chosen as randomization sites. In the case of library-A, the equivalent residues in PAMO were targets of mutagenesis in previous studies.[23,24] While we were generating these mutants, the crystal structure of *Rhodococcus* sp. HI-31 CHMO in complex with ε-caprolactone and $NADP^+$ ($RhCHMO_{Tight}$; PDB ID: 4RG3) was solved.[25] In the $RhCHMO_{Tight}$ crystal structure, ε-caprolactone is bound in an analogous position to that of MES in the WT PAMO crystal structure. Figure 1 shows the position in the AcCHMO active site of several residues mutated in the present work and ε-caprolactone, based on a superimposition of the WT AcCHMO model and the $RhCHMO_{Tight}$ crystal structure (RMSD = 0.48).

**Whole Cell Screening.** The Baeyer-Villiger oxidation of 2-butanone catalyzed by AcCHMO was first investigated using whole cells of *Escherichia coli* expressing the WT enzyme and its mutants. Whole cell biotransformations are generally preferred over purified enzyme reactions in industrial applications. In addition, this approach greatly simplifies the screening of large libraries in the laboratory. Previously, we confirmed that *E. coli* cells do not produce esterases or other enzymes with activity on either ethyl acetate or methyl propanoate under similar conditions to those used here.[15] Culture medium containing the expression inducer and 2-butanone was added to each well of a 96-square well plate prior to inoculation. After 24 h of incubation of these cultures, formation of ethyl acetate and methyl propanoate was determined in air samples collected from the headspace of each well using GC-MS.

30–100 *E. coli* colonies were screened per randomization site using NNK codon degeneracy.[26] Four hits showing an improvement in the desired regioselectivity were identified in library-A (**Table S1**). Cultures expressing the L244R, F281H, L435N, and I491A variants produced 30 to 40% methyl propanoate (percentage of total product), while the WT enzyme produced 26% methyl propanoate (**Table 1**). Library-B resulted in the identification of the T56S mutant which exhibits a higher activity on 2-butanone. The T56S mutant converted 92% of 2-butanone compared to 52% for the WT AcCHMO in 24 h (**Table 1**). Other AcCHMO mutants obtained at positions 56, 244, 281, 435, and 491 were not better than those described above (**Table S2**). Additional beneficial mutations were not found in library-C.

To obtain a mutant improved in both regioselectivity and activity on 2-butanone, the best mutations found in library-A were combined with the hit found in library-B (**Table 1**). The double mutants T56S/L244R and T56S/I491A presented a combination of the desired properties observed in the corresponding single mutants. The triple mutant T56S/L244R/I491A did not show an increase in the formation of either total product or methyl propanoate when compared to the T56S/I491A variant. The best regioselectivity was found for the T56S/L435N/I491A mutant. This triple mutant produced 49% methyl propanoate compared to 43% for the T56S/I491A variant. However, the T56S/L435N/I491A mutant produced less total product than the WT AcCHMO. This is in contrast to the T56S/I491A and the T56S/L244R mutants, which produce the most methyl propanoate when comparing absolute amounts.

**Table 1. Conversion of 2-Butanone and Production of Methyl Propanoate by AcCHMO[a]**

| AcCHMO | Conversion (%)[b] | | Mpr (%)[c] | |
|---|---|---|---|---|
| | Cells | E | Cells | E |
| WT | 52 | 48 | 26 | 24 |
| T56S | 92 | 85 | 26 | 24 |
| L244R | 55 | 53 | 32 | 28 |
| F281H | 52 | 33 | 30 | 27 |
| L435N | 13 | 8 | 33 | 35 |
| I491A | 35 | 25 | 40 | 34 |
| T56S/L244R | 88 | 79 | 29 | 29 |
| T56S/I491A | 73 | 59 | 43 | 39 |
| T56S/L244R/I491A | 67 | 56 | 43 | 39 |
| T56S/L435N/I491A | 40 | 34 | 49 | 51 |

[a]Analyses were carried out by headspace GC-MS after 24 h of *E. coli* culture expressing CHMO at 24 °C (cells) or after reacting purified enzyme (2 μM) for 5.5 h at 25 °C and pH 7.0 (E). The standard deviation for the conversion values is ≤17% and that for the yields of methyl propanoate is ≤6%. It is based on two or three replicates. [b]Relative to the initial concentration of 2-butanone (11 mM). [c]Yields of methyl propanoate are given in percentage of total product.

**Reactions Using Purified AcCHMO.** Small scale conversions of 2-butanone (11 mM) were carried out using purified AcCHMO fused to the NADPH regeneration enzyme phosphite-dehydrogenase (PTDH; 2 μM).[27,28] Fusing PTDH to AcCHMO has not significant adverse effects, based on previous kinetic studies and regio- and stereoselective transformations.[27,28] The reactions contained the purified WT AcCHMO or one of the mutants identified by whole cell screening (T56S, L244R, F281H, L435N, I491A, T56S/L244R, T56S/I491A, T56S/L244R/I491A, and T56S/L435N/I491A). In general, the results obtained by using purified AcCHMOs were in perfect agreement with those achieved using whole cells (**Table 1**). All variants exhibited a better regioselectivity toward methyl propanoate (28–51% methyl propanoate) than the WT enzyme (24% methyl propanoate), except for the T56S variant. Yet, the latter variant produced the highest amount of total product.

To study the effect of reaction conditions on the regioselectivity and activity of AcCHMO, purified WT enzyme and several variants were used to convert 2-butanone at various temperatures and pH values (**Figure 2** and **Table S3**). In the case of the WT enzyme, the amount of total product at all pH values was 2-5-fold higher at 30 °C than that at 4 °C. The desired regioselectivity was slightly improved at 4 °C compared to that at 37 °C (1.5-fold). The amount of total product for the WT enzyme was lower at pH 6.0 than that at pH 7.0 and 8.5 at all temperatures (2–4-fold), while the regioselectivity was pH independent. Similar trends were observed for all mutants.

In all reactions of purified AcCHMO with 2-butanone, the amount of total product obtained at 30 °C was similar or higher to that obtained at 37 °C (**Figure 2** and **Table S3**). This is probably caused by an increase in enzyme inactivation at higher temperatures. Previous studies have shown that the relatively low stability of AcCHMO limits its use as an industrial biocatalyst,[29] and great efforts are being made to address this issue.[21,30] We compared the thermostability of WT AcCHMO and the mutants using the ThermoFAD method.[31] The melting temperatures ($T_m$) values for these enzymes at pH 7.0 ranged from 29 °C to 40 °C, being 37 °C for WT AcCHMO (**Table S4**). The mutants T56S, I491A, T56S/I491A and T56S/L435N/I491A, which are the best mutants based on activity and/or regioselectivity, had even a slightly higher $T_m$ value than the WT enzyme (1–3 °C higher at pH 7.0). The effect of pH on the $T_m$ values was also investigated. In all enzymes, the $T_m$ values were slightly lower at pH 6.0 than at pH 7.0 and 8.5 (1–3 °C). This correlates with the effect of pH on 2-butanone conversion yield.

The effect of various salt concentrations (0.1–0.8 M KCl) on the reaction of purified WT AcCHMO with 2-butanone was also investigated, since a previous study showed that salts improve AcCHMO stability.[29] A negative correlation was found between KCl concentration and conversion yields (**Figure S1**). The amount of total product decreased from 46% to 16% by adding 0.8 M KCl to the reactions. In contrast, the addition of KCl did only slightly affect the enzyme regioselectivity.

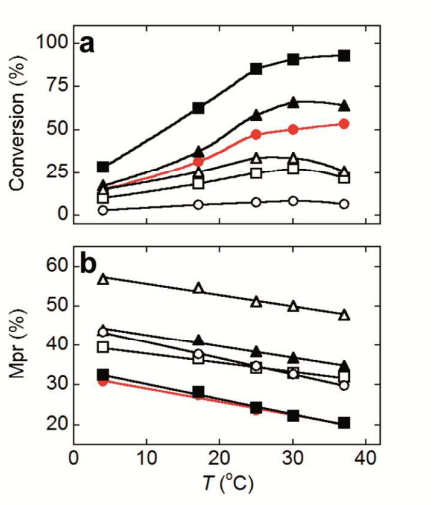


**Figure 2.** Conversion of 2-butanone and production of methyl propanoate by purified AcCHMO. WT (●), T56S (■), L435N (○), I491A (□), T56S/I491A (▲), T56S/L435N/I491A (△) AcCHMOs. Reaction contained 2 μM AcCHMO fused to PTDH, 11 mM 2-butanone, 150 μM NADPH, 50 mM Tris-HCl, pH 7.0, and 20 mM phosphite. Analyses were carried out by headspace GC-MS after 5.5 h of incubation.

Besides 2-butanone, 3-methyl-3-buten-2-one was assayed as substrate for the purified WT AcCHMO and its single mutants T56S and I491A. The abnormal product resulting from the Baeyer-Villiger oxidation of 3-methyl-3-buten-2-one is methyl methacrylate, which can be directly polymerized to form the acrylic plastic poly (methyl methacrylate). However, Figure S2 shows that exclusively the normal product isopropenyl acetate was detected in all reactions. Therefore, AcCHMO exhibits a different regioselectivity with 3-methyl-3-buten-2-one and 2-butanone. This result may due to the fact that 3-methyl-3-buten-2-one presents a larger difference in nucleophilic strength between the two carbons adjacent to the substrate carbonyl group than 2-butanone. Steric effects may also play a role in controlling the different regioselectivity of these reactions.

**Steady-State Kinetics.** To further characterize the reaction of WT AcCHMO and its mutants with a ketone substrate, steady-state kinetic studies were carried out at 25 °C and pH 7.0. Reactions were run under atmospheric dioxygen concentration (0.253 mM), which is saturating based on previous studies.[4,5] Table S5 shows the $k_{cat}$ values obtained for WT AcCHMO and its mutants with 2-butanone as a substrate. These values were determined by following

the decrease in absorbance of NADPH at 340 nm. The T56S mutant presented the highest $k_{cat}$ value (0.5 $s^{-1}$), which was 1.7-fold higher than that determined for the WT AcCHMO (0.3 $s^{-1}$) (**Figure 3, panel a**). This is in agreement with the conversion data; the amount of total product was doubled in the reactions using the T56S mutant compared to WT AcCHMO. The other mutants presented $k_{cat}$ values of 0.2–0.4 $s^{-1}$ (**Figure S3**). The $K_{m(2\text{-butanone})}$ values for WT AcCHMO and the T56S mutant were 2.4 mM and 0.7 mM, respectively. The T56S/L244R mutant presented the same $K_{m(2\text{-butanone})}$ value as that obtained for the T56S mutant. In the case of the other mutants, the $K_{m(2\text{-butanone})}$ value could not be determined since the $k_{cat}$ values with 2-butanone are similar to the uncoupling rates (**Table S5** and **Figure S3**). Using cyclohexanone as a substrate, the WT AcCHMO and the T56S mutant presented the same $k_{cat}$ values (6 $s^{-1}$) and similar $K_m$ values (9 and 4 μM, respectively). Clearly, AcCHMO has evolved to become an efficient biocatalyst to convert cyclohexanone and the T56S mutation has only a marginal effect on the efficiency with cyclohexanone.

The effect of pH on the uncoupling rate was studied. For effective monooxygenase-catalyzed conversions, uncoupling should be minimized. Figure 3 (**panel b**) shows that the uncoupling rate for the WT enzyme is 6-fold lower at pH 6.0 than at pH 9.0. This observation is in line with previous studies on WT AcCHMO which revealed that the C4a-peroxyflavin is less stable at pH 9.0 than at 7.0 in the absence of the substrate.[4] The same effect of pH on the stability of the C4a-peroxyflavin intermediate was observed for liver microsomal flavin-containing monooxygenase,[32] the monooxygenase component (C2) of *p*-hydroxyphenylacetate-3-hydroxylase,[33] and a siderophore-associated flavin-containing monooxygenase.[34] Experimental and computational studies have shown that the active site environment controls the stability of the C4a-peroxyflavin intermediate.[35] Its decay rate is influenced by the protonation state of active site residues or ligands, which is modulated by pH changes. Figure 3 (**panel b**) shows that the T56S mutant presents the same or lower uncoupling rate than that for the WT enzyme at the assayed pH values. Intriguingly, the pH had no significant effect on the uncoupling rate for this mutant, suggesting that its active site environment is different to that of WT AcCHMO.

Flavin-containing monooxygenases produce little or no hydrogen peroxide during catalysis with adequate substrates. Yet, significant production of hydrogen peroxide in the presence of non-optimal substrates has been observed.[34] We measured the rate of hydrogen peroxide formation for WT AcCHMO and the T56S mutant in the presence of various concentrations of 2-butanone using a coupled assay with horseradish peroxidase. Figure 3 (**panel a**) shows the rates obtained using this method in comparison to those determined by following the consumption of NADPH. In both WT AcCHMO and the T56S mutant, the rate of hydrogen peroxide production decreased in the presence of 2-butanone. For example, the rate of hydrogen peroxide production for the WT AcCHMO was 0.05 $s^{-1}$ in the presence of 30 mM 2-butanone, while it was 0.1 $s^{-1}$ in the absence of a ketone substrate. The hydrogen peroxide produced during catalysis of WT AcCHMO with 2-butanone has no effect on the yield of ethyl acetate and methyl propanoate, since the results did not vary by adding catalase (1 and 50 U) to reactions with 2-butanone at pH 7.0 and 8.5 (**Table S6**).

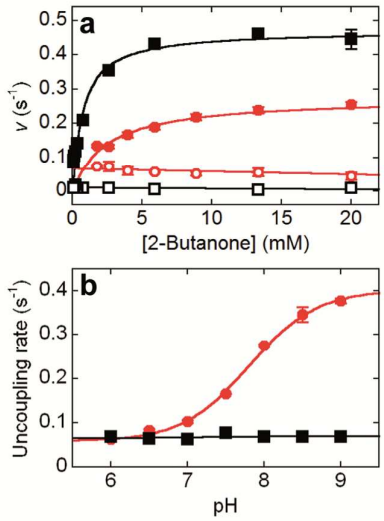


**Figure 3.** Steady-state kinetics with 2-butanone (panel a) and uncoupling rate (panel b) for WT (●/○) and T56S (■/□) AcCHMOs. Rate values were determined at 25 °C by following either the NADPH consumption (full symbols) or the hydrogen peroxide production (open symbols). Reactions contained 4 μM AcCHMO fused to PTDH, 150 μM NADPH, and 0.253 mM dioxygen. Buffers at pH 7.0 (panel a) or pH 6.0–9.0 (panel b) were used.

**Enzyme-monitored Turnover.** To investigate which reaction step limits the AcCHMO turnover rate, enzyme-monitored turnover experiments were carried out using a stopped-flow spectrophotometer (pH 7.0, 25 °C, and 0.253 mM dioxygen). In the presence of WT enzyme (15 μM) and NADPH (200 μM), a low absorbance at 440 nm was measured during the steady-state period ($A_{440}$ = 0.04; 17% of the fully oxidized FAD absorbance; **Figure S4, panel a**). When all NADPH was consumed, as evidenced by a low and stable absorbance at 340 nm, full enzyme reoxidation was observed. In the enzyme reaction containing 2-butanone (50 mM) or cyclohexanone (0.25 mM), together with NADPH (200 μM), the absorbance was found to be 35% and 46% of the fully oxidized flavin absorbance, respectively (**Figure S4**). These observations indicate that the overall turnover is mainly governed by one of the steps in the catalytic cycle occurring after enzyme reduction in the absence and the presence of the ketone substrate (**Scheme 1**). This was further investigated as described below.

**Reductive Half-reaction.** The T56S and I491A AcCHMO mutants exhibit an improvement in activity and the desired regioselectivity, respectively, as compared to those for the WT enzyme. To identify the specific reaction steps affected by the mutations, we carried out pre-steady state kinetic studies using a stopped-flow spectrophotometer.

The reductive half-reaction for WT AcCHMO and the T56S and I491A mutants was monitored by following the decrease in absorbance at 440 nm due to the reduction of enzyme-bound FAD under anaerobic conditions. The stopped-flow traces at various NADPH concentrations (62–150 μM) were fit with a double exponential function, with a fast phase accounting for 64%, 82%, and 90% of the absorption change for the WT AcCHMO, T56S mutant, and I491A mutant, respectively (**Figure 4, panel a**). Previously, similar stopped-flow traces were observed for the anaerobic reaction of PAMO with NADPH.[6] It was suggested that the fast phase is due to the PAMO reduction, while the slow phase may be due to the formation of a small amount of C4a-peroxyflavin intermediate in the presence of residual traces of dioxygen.[6] In WT AcCHMO and the mutants, the observed rate for each phase ($k_{obs1}$ and $k_{obs2}$) was constant at all assayed NADPH concentrations. Accordingly, the $K_{d(NADPH)}$ value for WT AcCHMO was previously estimated to be 7.0 μM.[4] Both $k_{obs1}$ and $k_{obs2}$ values for the WT AcCHMO were significantly higher than those for the T56S and I491A mutants. The calculated $k_{red1}$ values for WT, T56S, and I491A AcCHMOs are 169, 69, and 25 $s^{-1}$, respectively (**Figure 4, panel b**). The reduction of the FAD bound to AcCHMO is not the main rate-limiting step in the reaction with 2-butanone since the $k_{red1}$ value is significantly higher than the $k_{cat}$ value in all cases (**Table S5**). These results are in accordance with those described above for the enzyme-monitored turnover experiment with WT AcCHMO.

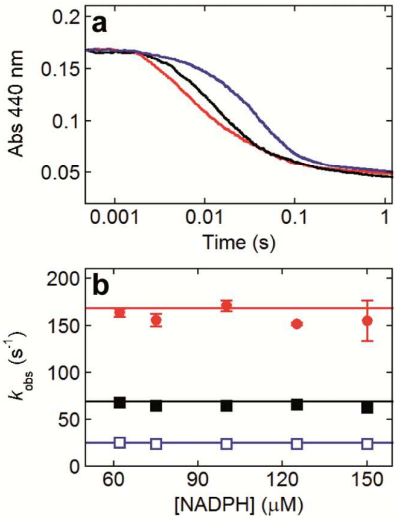


**Figure 4.** Reductive half-reaction of WT (●), T56S (■), and I491A (□) AcCHMO. All reactions contained 12 μM AcCHMO fused to PTDH, 50 mM Tris-HCl, pH 7.0, at 25 °C under anaerobic conditions. In panel a, stopped-flow traces with 62 μM NADPH are shown.

**Oxidative Half-reaction.** The oxidative-half reaction for AcCHMO was investigated using the stopped-flow spectrophotometer in double-mixing mode. The enzyme was first anaerobically reduced with 1.2 equivalents of NADPH in the aging loop of the stopped-flow apparatus. The reduction time was 5 s for the WT enzyme and 10 s for the mutants. The anaerobically reduced enzyme was subsequently mixed with air-saturated buffer in the absence or the presence of 2-butanone.

The first spectrum after mixing the anaerobically reduced WT AcCHMO with air-saturated buffer shows a maximum at 366 nm (**Figure 5, panel a**). Subsequently, a fast increase in the absorbance at 366 nm was observed during 0.01 s. A second intermediate with a maximum at 379 nm was also observed, with a formation rate of 36 $s^{-1}$ and decay rate of 0.05 $s^{-1}$. Finally, an absorbance increase at 440 nm consistent with the hydrogen peroxide elimination to form the reoxidized enzyme ($k$ = 0.08 $s^{-1}$) was observed. The enzyme reoxidation rate was similar to the uncoupling rate (0.11 $s^{-1}$). Similar results were obtained when this experiment was carried out with the AcCHMOs mutants (**Figure 5, panel b and c**). However, the second intermediate of the mutants has an absorbance maximum at 370 nm. It was previously suggested for WT AcCHMO that the first enzyme intermediate contains C4a-peroxyflavin, which is protonated to form C4a-hydroperoxyflavin.[4] Alternatively, the protonation of an enzyme residue may influence the spectral properties of the C4a-peroxyflavin intermediate.[4]

After mixing the anaerobically reduced AcCHMO with 60 mM 2-butanone in air-saturated buffer, a rapid increase in absorbance at 366 nm due to the formation of the C4a-peroxy-FAD intermediate was observed (**Figure 5, panel d-f**). Subsequently, a decrease in absorbance at 366 nm together with an increase in absorbance at 440 nm was observed. The stopped-flow traces at 440 nm, obtained in the presence of 2-butanone, were fit to a single exponential function. The resulting rates for the WT, T56S, and I491A AcCHMOs were 0.3, 0.6, and 0.1 $s^{-1}$, respectively (**Figure S5**). Similar values were obtained by fitting the stopped-flow traces at 366 nm to obtain the rate of intermediate decay (**Figure S5**). These values are also similar to the $k_{cat}$ values for AcCHMO with 2-butanone (**Table S5**). These experiments show that the decay of the C4a-peroxy-flavin intermediate to form the oxidized enzyme is faster for the T56S AcCHMO mutant than for the WT enzyme in the presence of 2-butanone. Before the C4a-peroxy-flavin intermediate decay, several steps occur in the enzyme reaction with 2-butanone (**Scheme 1**): i) 2-butanone binding; ii) formation and rearrangement of the Criegee intermediate; iii) formation of C4a-hydroxyflavin; and iv) elimination

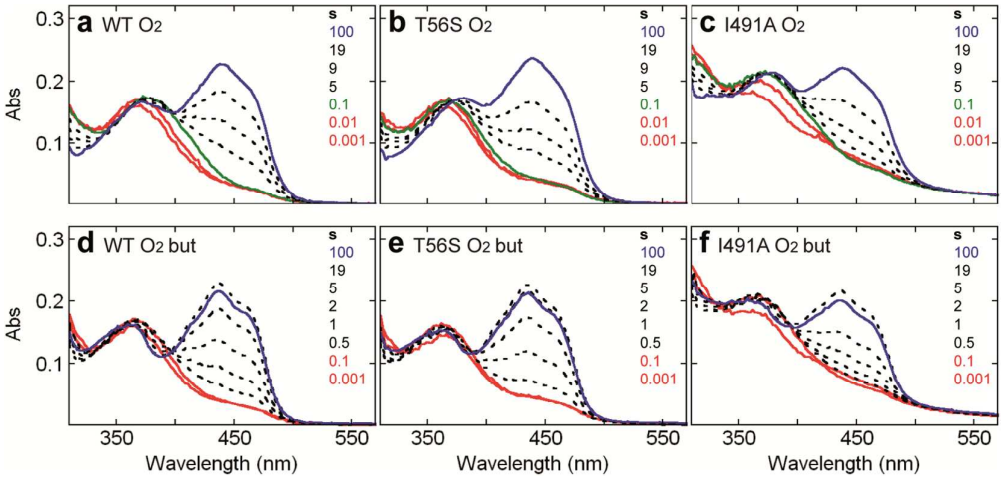


**Figure 5.** Spectral changes observed during the oxidative half-reaction of WT, T56S, and I491A AcCHMOs. Anaerobically reduced AcCHMO (1.2 equivalents NADPH/1 CHMO) was mixed with air-saturated buffer with or without 2-butanone in 50 mM Tris-HCl, pH 7.0, at 25 °C (60 mM 2-butanone, 18/17 μM CHMO fused to PTDH, final concentrations).

of a water molecule. Additional experiments are required to clarify which of these steps is improved in the T56S mutant compared to the WT enzyme.

**Importance of T56, L435, and I491 Residues in AcCHMO.** The results presented above show that the residues located at positions 56, 435, and 491 in AcCHMO are important for the reaction of this enzyme with 2-butanone. In the case of WT AcCHMO, a conversion yield of 48% was determined using the purified enzyme. Under the same conditions, almost full conversion of 2-butanone was achieved by the T56S AcCHMO mutant. In comparison to the WT AcCHMO, the T56S mutant enzyme has a higher turnover number with 2-butanone due to a higher rate of flavin reoxidation. In addition, the T56S AcCHMO mutant has a lower uncoupling rate than the WT AcCHMO (**Table S5**). Replacement of T56 with serine reduced (2-fold) the anaerobic rate of flavin reduction at saturating NADPH concentration. This shows that T56 is involved in both the AcCHMO reductive and oxidative half-reactions. A multiple sequence alignment of characterized CHMOs showed that all other CHMOs have a serine residue at the equivalent position to that of T56 in AcCHMO (**Figure S6**). Figure 1 shows that the AcCHMO T56 is located at 5 Å from the flavin N5, on the flavin *si*-side, but the side chain of this residue is pointing away from the isoalloxazine ring. The same side chain position is observed for the equivalent serine in the available CHMOs crystal structures.

In a similar position to that of AcCHMO T56, most flavoenzymes have a hydrogen-bond donor located within hydrogen-bond distance to the flavin N5 atom.[36] In the oxygenase component of *p*-hydroxyphenylacetate-3-hydroxylase, the C4a-hydroperoxyflavin intermediate is stabilized via a H-bond interaction between the flavin N5 atom and the S171 (equivalent to AcCHMO T56).[37] In pyranose 2-oxidase, a C4a-hydroperoxyflavin intermediate was not detected during the oxidative half-reaction when the T169 (equivalent to AcCHMO T56) was replaced with other residues.[38] Other examples of flavoenzymes harboring a serine or threonine in a similar position are alditol oxidase (S106; PDB ID: 2VFS),[39] choline oxidase (S101; PDB ID: 4MJW),[40] and electron-transfer flavoprotein from the methylotrophic bacterium W3A1 (S254; PDB ID: 1O97).[41] The sequence-related PAMO harbors C65 at the equivalent position of T56 in AcCHMO. It has been shown that in the C65D PAMO mutant, the rate of decay of the C4a-peroxyflavin intermediate is significantly increased compared to that for the WT PAMO.[42] As a result, the uncoupling rate for this mutant was 5.0 $s^{-1}$ while it is only 0.02 $s^{-1}$ for the WT PAMO.[42] Based on available crystal structures, other BVMOs present either a cysteine or a residue with a non-polar side chain at the equivalent position to that of T56 in AcCHMO.

The residue adjacent to T56 in AcCHMO, D57, is strictly conserved among all known CHMOs. Based on available BVMO crystal structures, this is a mobile residue that participates in the positioning of the NADPH via a hydrogen bond interaction with the nicotinamide base.[22,43] In AcCHMO, the replacement of the T56 residue with serine might result in small changes in the position of the D57 residue that improve the reaction with 2-butanone. Alternatively, the T56 side chain could rotate to interact with the flavin N5 atom during the reaction. As a result of this rotation, the T56 side chain would achieve a similar

position to that of PAMO C65 side chain, which is located at 4.5 Å from the flavin N5 atom.

Based on the 2-butanone conversions presented here, the I491A AcCHMO mutant presents a better regioselectivity toward methyl propanoate than that for the WT enzyme (**Table 1**). AcCHMO I491 is located on a mobile loop formed by residues 485–502. Based on available CHMOs crystal structures, changes in the position of this loop modulate the solvent accessibility to the substrate binding site.[25] Replacement of the equivalent residue in PAMO (Y502) with an alanine did not affect the $k_{cat}$ value while the $K_{m(phenylacetone)}$ value was 20-fold increased and the enantioselectivity was also influenced.[23] The adjacent residue to AcCHMO I491, W490, is strictly conserved among all known BVMOs. The equivalent residue in RhCHMO, W492, interacts with the $NADP^+$ ribose during the catalytic cycle.[43] In comparison with the WT RhCHMO, the W492A mutant presented low activity, high uncoupling rate, and altered selectivity.[25,43] The equivalent mutant for PAMO, W501A, has a lower $k_{cat}$, a higher $K_{m(phenylacetone)}$, and a higher uncoupling rate than the WT enzyme.[23]

The L435N AcCHMO mutant exhibited an improvement in the desired regioselectivity compared to that for the WT AcCHMO (**Table 1**). However, the yield of total product for the L435N mutant was 6-fold lower than that for the WT AcCHMO. Similar trends were observed when the T56S/L435N/I491A mutant was compared to the T56S/I491A mutant. Figure 1 shows that the L435N is located at ~5 Å from the substrate, based on a superimposition of AcCHMO homology model and RhCHMO crystal structure. The structure of PAMO in complex with MES shows that the equivalent residue to AcCHMO L435 (M446) interacts with the ligand.[22] The M446G PAMO mutant had a different substrate specificity and enantioselectivity compared to the WT PAMO.[44]

**Conclusions.** *E. coli* cells expressing WT AcCHMO convert 52% 2-butanone after 24 h at 24 °C resulting in the formation of 26% methyl propanoate of the total product formed. This ester is of industrial interest as it can be used as a precursor of acrylic plastic. As a result of the present study, the T56S/I491A AcCHMO mutant was obtained. It exhibits a significant improvement in both 2-butanone conversion yield (73%) and the desired regioselectivity (43% methyl propanoate) compared to those for WT AcCHMO. These results were confirmed using purified enzyme. Interestingly, the T56S mutation not only improved the rate of catalysis but also significantly lowered the uncoupling rate. This shows that by enzyme engineering such futile catalytic activity of BVMOs can be reduced. Several other mutations were found to influence the regioselectivity of AcCHMO when acting on the smallest asymmetric aliphatic ketone, 2-butanone. This demonstrates that subtle changes in the active site environment (i.e., replacement of AcCHMO I491 with alanine) can influence the enzyme regioselectivity for such relatively small substrate. Additional engineering studies are desirable to further improve the regioselectivity of AcCHMO with 2-butanone with the aim of using this reaction in industry. We anticipated that it is not an easy task and thus the implementation of an efficient method to separate methyl propanoate from ethyl acetate should be also considered.

# METHODS

**Materials.** NADPH was acquired from Jülich Chiral Solutions GmbH. All other materials were acquired from Sigma-Aldrich unless otherwise specified.

**Generation of Mutants.** The pCRE2-CHMO construct[28] was used as a template to generate the AcCHMO mutants. This construct harbors a gene encoding WT AcCHMO fused to the C-terminus of PTDH. A His-Tag at the N-terminus of the PTDH is also included in this construct. Site saturation mutagenesis was carried out as previously described,[21] using NNK codons instead of single codons. Single *E. coli* colonies harboring the plasmids encoding the AcCHMO mutants were picked and grown in 250 µL Luria-Bertani medium containing 50 µg/ml ampicillin (LB-amp) in 2 mL deep 96-square well plates (Waters) covered by adhesive seals (AeraSeal film, Excel Scientific). 100 µL of this culture was mixed with 50 µL 60% (v/v) glycerol in 96-well microplates (U-shape, greiner bio-one) and frozen at –80 °C.

**Screening of Mutants.** 250 µL LB-amp was added to each well of a 2 mL deep 96-square well plate prior to inoculation of the *E. coli* cells containing the plasmids encoding the AcCHMO mutants. Inoculation was carried out using glycerol stocks frozen in a 96-well microplate and a cryo-replicator press (CR1100, EnzyScreen). After 24 h of incubation at 30 °C and 1,050 rpm (Titramax 1000 incubator, Heidolph), 20 µL from each culture were transferred into the wells of a 2 mL deep 96-square well plate. Subsequently, 180 µL LB-amp containing 0.02% (w/v) L-arabinose and 11 mM 2-butanone was added to each well and the plates were covered with a polypropylene cap mat (Waters). After 24 h of incubation at 17 °C or 24 °C and 1,050 rpm, analyses were carried out by headspace GC-MS as described below.

**Expression and Purification.** WT AcCHMO and its mutants, fused to PTDH and a His-Tag, were expressed and purified as previously described[21] with the following modifications: i) L-arabinose was added to the expression medium before the inoculation; ii) after the inoculation, the cultures were incubated 40 h at 24 °C; iii) 10 µM FAD was not added to the lysis buffer; and iv) 2 mL of Ni-sepharose resin was used for each 50 mL culture. For all experiments described in this work, purified enzyme concentration was determined based on the extinction coefficient of WT AcCHMO at 440 nm (13.8 $mM^{-1}$ $cm^{-1}$).[45]

**Reactions of Purified AcCHMO with a Ketone Substrate.** Purified WT AcCHMO and its variants (2 µM) were reacted with 2-butanone (11 mM) at various

temperatures (4, 17, 25, 30, and 37 °C) and pH values (6.0, 7.0, and 8.5). In the case of WT AcCHMO, the effect of various KCl concentrations (0.1, 0.3, 0.6, and 0.8 M) and catalase (1 and 50 U) on the reaction with 2-butanone (11 mM) at 25 °C and pH values of 7.0 and 8.5 was also studied. Similarly, 3-methyl-3-buten-2-one (10 mM) was assayed as substrate for the purified WT AcCHMO and the T56S and I491A mutants (10 μM) at pH 7.0, 24 °C, and 135 rpm. All reactions contained 150 μM NADPH, 20 mM phosphite, and either 50 mM Tris-HCl (pH 7.0 and 8.5) or 50 mM sodium phosphate (pH 6.0). A final reaction volume of 0.5 mL was prepared in a 20 mL vial (headspace, screw top, Agilent). The reaction time was 5.5 h when 2-butanone was used as a substrate, while 24 h incubations were carried out for the reactions containing 3-methyl-3-buten-2-one. Reactions were stopped by incubation at 60 °C for 10 min. Analyses were carried out by headspace GC-MS as described below.

**Headspace GC-MS Analysis.** Reactions of AcCHMO with the ketone substrates were analyzed by headspace GC-MS using a GCMS-QP2010 (Shimadzu) in an air-conditioned room (21 °C). A HP-1 column (30 m x 0.25 mm x 0.25 μm, Agilent) was used. 250 μL headspace samples were injected. The injector temperature was set at 150 °C. The temperature programs used for the different reactions are as follows: i) for the screening in 96-square well plates, isothermic at 35 °C for 1.7 min; ii) for the reactions of purified enzyme with 2-butanone in vials, isothermic at 35 °C for 3.3 min; and iii) for the reactions of purified enzyme with 3-methyl-3-buten-2-one in vials, isothermic at 35 °C for 5 min, and then from 35 °C to 150 °C at 20 °C/min. Reactions prepared in vials were stirred at 40 °C for 2.5 min before the analysis. Standards were used to identify the substrates and products by retention time and their characteristic fragmentation pattern. Calibration curves of 2-butanone, ethyl acetate, and methyl propanoate were carried out to quantify these compounds in the reactions.

**Determination of Melting Temperatures.** The melting temperature values for purified WT AcCHMO and various mutants of this enzyme, fused to PTDH and a His-Tag, were determined using the ThermoFAD method as previously described.[31] For these assays, 10 μM enzyme was prepared in 50 mM Tris-HCl, pH 7.0 or 8.5, or 50 mM sodium phosphate, pH 6.0.

**Steady-State Kinetics.** Steady-state kinetic parameters for purified WT AcCHMOs and its mutants were determined using a spectrophotometer. Enzyme (4 μM), NADPH (150 μM), and various 2-butanone concentrations were reacted in 50 mM Tris-HCl pH 7.0, at 25 °C, and atmospheric dioxygen concentration. In these reactions, the rate of NADPH consumption was determined by following the decrease in absorbance at 340 nm ($\varepsilon_{340}$ = 6.22 $mM^{-1}$ $cm^{-1}$). Alternatively, the increase in absorbance at 515 nm ($\varepsilon_{515}$ = 26 $mM^{-1}$ $cm^{-1}$) was measured to determine the rate of hydrogen peroxide production in the presence of horseradish peroxidase (4 U), 4-aminoantipyrine (0.1 mM), and 3,5-dichloro-2-hydroxybenzenesulfonic acid (1.0 mM). The NADPH consumption assay was also carried out using cyclohexanone instead of 2-butanone as a substrate and 0.01–0.05 μM AcCHMO. The initial rates of the reactions were plotted as a function of the ketone substrate concentrations. These data were fit to the Michaelis-Menten equation using the software KaleidaGraph (Synergy Software, Reading, PA).

**Enzyme-monitored Turnover.** Enzyme-monitored turnover experiments were carried out using a SX20 stopped-flow spectrometer (Applied Photophysics, Surrey, UK) in single-mixing configuration. WT AcCHMO (15 μM) was reacted with NADPH (200 μM) and 2-butanone (50 mM) in 50 mM Tris-HCl at pH 7.0, 25 °C, and atmospheric dioxygen concentration. The absorbance of both the FAD bound to AcCHMO and the NADPH was monitored at 440 and 340 nm, respectively. For comparison, the same experiment was carried out in the absence of 2-butanone or in the presence of cyclohexanone (0.25 mM) instead of 2-butanone. A control reaction without both NADPH and a ketone substrate was also assayed.

**Rapid Kinetics.** The catalytic cycle of WT AcCHMO and its mutants was studied using a SX20 stopped-flow spectrometer. The single- and double-mixing mode of this apparatus was used to investigate the enzyme reductive and oxidative half-reactions, respectively. A xenon lamp and either a photomultiplier tube (PMT) detector or a photodiode array (PDA) detector were used. The age of the reaction of the mixed reagents in the observation cell is 1 millisecond (dead-time) when the data acquisition starts. All experiments were carried out in 50 mM Tris-HCl at pH 7.0 and 25 °C. All assays were run in duplicate or triplicate by mixing equal volumes of reactants.

The enzyme reduction was performed in the absence of dioxygen. To make the stopped-flow spectrometer anaerobic, the flow-circuit of this apparatus was repeatedly washed with anaerobic buffer. Anaerobic solutions (2 or 4 mL) were prepared in gastight glass syringes (5 or 10 mL, Hamilton, Nevada, USA). NADPH and buffer solutions were made anaerobic by bubbling argon through the solutions for 10 min. To deoxygenate the enzyme solution, argon was blown on the surface of the solution for 10 min. *Aspergillus niger* glucose oxidase (Sigma-Aldrich) and glucose were added to the solutions to remove any residual traces of dioxygen (final concentrations 0.5 μM and 2 mM, respectively).

All data were analyzed using the software Pro-Data and Pro-K (Applied Photophysics, Surrey, UK) or KaleidaGraph (Synergy Software, Reading, PA). Stopped-flow traces were fit to the corresponding exponential function to determine the observed rates ($k_{obs}$).

# ASSOCIATED CONTENT

*Supporting Information Available*: This material is available free of charge *via* the Internet.

Tables S1–S6 and Figures S1–S6.

# AUTHOR INFORMATION

**Corresponding Author**
*E-mail: m.w.fraaije@rug.nl

**Notes**
[ϕ]Current address: Forschungszentrum Jülich GmbH, Jülich, Germany
[§]These authors contributed equally to this work.
The authors declare no competing financial interest.

## ACKNOWLEDGEMENTS

This work has been supported by the Methyl Esters from Biomass grant (MEBIO; 053.24.105) from the Netherlands Organisation for Scientific Research (NWO).

## REFERENCES

(1) Leisch, H., Morley, K., and Lau, P. C. K. (2011) Baeyer-Villiger monooxygenases: more than just green chemistry, *Chem. Rev. 111*, 4165–4222.

(2) de Gonzalo, G., Mihovilovic, M. D., and Fraaije, M. W. (2010) Recent developments in the application of Baeyer-Villiger monooxygenases as biocatalysts, *ChemBioChem 11*, 2208–2231.

(3) Reignier, T., de Berardinis, V., Petit, J. L., Mariage, A., Hamzé, K., Duquesne, K., and Alphand, V. (2014) Broadening the scope of Baeyer-Villiger monooxygenase activities toward $\alpha$, $\beta$-unsaturated ketones: a promising route to chiral enol-lactones and ene-lactones, *ChemComm 50*, 7793–7796.

(4) Sheng, D., Ballou, D. P., and Massey, V. (2001) Mechanistic studies of cyclohexanone monooxygenase: chemical properties of intermediates involved in catalysis, *Biochemistry 40*, 11156–11167.

(5) Ryerson, C. C., Ballou, D. P., and Walsh, C. (1982) Mechanistic studies on cyclohexanone oxygenase, *Biochemistry 21*, 2644–2655.

(6) Torres Pazmiño, D. E., Baas, B. J., Janssen, D. B., and Fraaije, M. W. (2008) Kinetic mechanism of phenylacetone monooxygenase from Thermobifida fusca, *Biochemistry 47*, 4082–4093.

(7) Kelly, D. R., Knowles, C. J., Mahdi, J. G., Taylor, I. N., and Wright, M. A. (1995) Mapping of the functional active site of Baeyer-Villigerases by substrate engineering, *J Chem Soc, Chem Commun 7*, 729–730.

(8) Polyak, I., Reetz, M. T., and Thiel, W. (2012) Quantum mechanical/molecular mechanical study on the mechanism of the enzymatic Baeyer-Villiger reaction, *J Am Chem Soc 134*, 2732–2741.

(9) Rioz‐Martínez, A., de Gonzalo, G., Torres Pazmiño, D. E., Fraaije, M. W., and Gotor, V. (2009) Enzymatic baeyer-villiger oxidation of benzo‐fused ketones: formation of regiocomplementary lactones, *Eur J Org Chem 15*, 2526–2532.

(10) Fink, M. J., Snajdrova, R., Winninger, A., and Mihovilovic, M. D. (2016) Regio-and stereoselective synthesis of chiral nitrilolactones using Baeyer-Villiger monooxygenases, *Tetrahedron 72*, 7241–7248.

(11) Balke, K., Schmidt, S., Genz, M., and Bornscheuer, U. T. (2016) Switching the regioselectivity of a cyclohexanone monooxygenase toward (+)-*trans*-dihydrocarvone by rational protein design, *ACS Chem Biol 11*, 38–43.

(12) Rehdorf, J., Lengar, A., Bornscheuer, U. T., and Mihovilovic, M. D. (2009) Kinetic resolution of aliphatic acyclic $\beta$-hydroxyketones by recombinant whole-cell Baeyer-Villiger monooxygenases-Formation of enantiocomplementary regioisomeric esters, *Bioorg Med Chem Lett 19*, 3739–3743.

(13) Rehdorf, J., Mihovilovic, M. D., and Bornscheuer, U. T. (2010) Exploiting the regioselectivity of Baeyer-Villiger monooxygenases for the formation of $\beta$‐amino acids and $\beta$‐amino alcohols, *Angew. Chem. Int. Ed. 49*, 4506–4508.

(14) Fraaije, M. W., Kamerbeek, N. M., Heidekamp, A. J., Fortin, R., and Janssen, D. B. (2004) The prodrug activator EtaA from *Mycobacterium tuberculosis* is a Baeyer-Villiger monooxygenase, *J Biol Chem 279*, 3354–3360.

(15) van Beek, H. L., Winter, R. T., Eastham, G. R., and Fraaije, M. W. (2014) Synthesis of methyl propanoate by Baeyer-Villiger monooxygenases, *Chem Commun 50*, 13034–13036.

(16) Harris, B. (2010) Acrylics for the future, *Ingenia 45*, 18–23.

(17) Yoneda, H., Tantillo, D. J., and Atsumi, S. (2014) Biological production of 2‐butanone in *Escherichia coli*, *ChemSusChem 7*, 92–95.

(18) Srirangan, K., Liu, X., Akawi, L., Bruder, M., Moo-Young, M., and Chou, C. P. (2016) Engineering *Escherichia coli* for microbial production of butanone, *Appl Environ Microbiol 82*, 2574–2584.

(19) Janssen, A. J. M., and Zwanenburg, B. (1991) PPL-catalyzed resolution of 1, 2-and 1, 3-diols in methyl propionate as solvent. An application of the tandem use of enzymes, *Tetrahedron 47*, 7409–7416.

(20) Poucher, W. A. (1991) *Poucher's perfumes, cosmetics and soaps*, Vol. 1, 9 ed., Chapman and Hall, London.

(21) van Beek, H. L., Wijma, H. J., Fromont, L., Janssen, D. B., and Fraaije, M. W. (2014) Stabilization of cyclohexanone monooxygenase by a computationally designed disulfide bond spanning only one residue, *FEBS Open Bio 4*, 168–174.

(22) Orru, R., Dudek, H. M., Martinoli, C., Torres Pazmiño, D. E., Royant, A., Weik, M., Fraaije, M. W., and Mattevi, A. (2011) Snapshots of enzymatic Baeyer-Villiger catalysis. Oxygen activation and intermediate stabilization, *J. Biol. Chem. 286*, 29284–29291.

(23) Dudek, H. M., Fink, M. J., Shivange, A. V., Dennig, A., Mihovilovic, M. D., Schwaneberg, U., and Fraaije, M. W. (2014) Extending the substrate scope of a Baeyer-Villiger monooxygenase by multiple-site mutagenesis, *Appl. Microbiol. Biotechnol. 98*, 4009–4020.

(24) Reetz, M. T., and Wu, S. (2009) Laboratory evolution of robust and enantioselective Baeyer-Villiger monooxygenases for asymmetric catalysis, *J Am Chem Soc 131*, 15424–15432.

(25) Yachnin, B. J., McEvoy, M. B., MacCuish, R. J. D., Morley, K. L., Lau, P. C. K., and Berghuis, A. M. (2014) Lactone-bound structures of cyclohexanone monooxygenase provide insight into the stereochemistry of catalysis, *ACS Chem. Biol. 9*, 2843–2851.

(26) Reetz, M. T., Kahakeaw, D., and Lohmer, R. (2008) Addressing the numbers problem in directed evolution, *ChemBioChem 9*, 1797–1804.

(27) Torres Pazmiño, D. E., Snajdrova, R., Baas, B. J., Ghobrial, M., Mihovilovic, M. D., and Fraaije, M. W. (2008) Self‐sufficient baeyer-villiger monooxygenases: effective coenzyme regeneration for biooxygenation by fusion engineering, *Angew Chem 120*, 2307–2310.

(28) Torres Pazmiño, D. E., Riebel, A., de Lange, J., Rudroff, F., Mihovilovic, M. D., and Fraaije, M. W. (2009) Efficient biooxidations catalyzed by a new generation of self - sufficient Baeyer-Villiger monooxygenases, *ChemBioChem 10*, 2595–2598.
(29) Zambianchi, F., Pasta, P., Carrea, G., Colonna, S., Gaggero, N., and Woodley, J. M. (2002) Use of isolated cyclohexanone monooxygenase from recombinant *Escherichia coli* as a biocatalyst for Baeyer-Villiger and sulfide oxidations, *Biotechnol. Bioeng. 78*, 489–496.
(30) Schmidt, S., Genz, M., Balke, K., and Bornscheuer, U. T. (2015) The effect of disulfide bond introduction and related Cys/Ser mutations on the stability of a cyclohexanone monooxygenase, *J. Biotechnol. 214*, 199–211.
(31) Forneris, F., Orru, R., Bonivento, D., Chiarelli, L. R., and Mattevi, A. (2009) ThermoFAD, a Thermofluor®-adapted flavin ad hoc detection system for protein folding and ligand binding, *FEBS J. 276*, 2833–2840.
(32) Jones, K. C., and Ballou, D. P. (1986) Reactions of the 4a-hydroperoxide of liver microsomal flavin-containing monooxygenase with nucleophilic and electrophilic substrates, *J Biol Chem 261*, 2553–2559.
(33) Ruangchan, N., Tongsook, C., Sucharitakul, J., and Chaiyen, P. (2011) pH-dependent studies reveal an efficient hydroxylation mechanism of the oxygenase component of *p*-hydroxyphenylacetate 3-hydroxylase, *J Biol Chem 286*, 223–233.
(34) Frederick, R. E., Ojha, S., Lamb, A., and DuBois, J. L. (2014) How pH modulates the reactivity and selectivity of a siderophore-associated flavin monooxygenase, *Biochemistry 53*, 2007–2016.
(35) Bach, R. D., and Mattevi, A. (2013) Mechanistic aspects regarding the elimination of $H_2O_2$ from C (4a)-hydroperoxyflavin. The role of a proton shuttle required for $H_2O_2$ elimination, *J Org Chem 78*, 8585–8593.
(36) Fraaije, M. W., and Mattevi, A. (2000) Flavoenzymes: diverse catalysts with recurrent features, *TIBS 25*, 126–132.
(37) Thotsaporn, K., Chenprakhon, P., Sucharitakul, J., Mattevi, A., and Chaiyen, P. (2011) Stabilization of C4a-hydroperoxyflavin in a two-component flavin-dependent monooxygenase is achieved through interactions at flavin N5 and C4a atoms, *J Biol Chem 286*, 28170–28180.
(38) Pitsawong, W., Sucharitakul, J., Prongjit, M., Tan, T.-C., Spadiut, O., Haltrich, D., Divne, C., and Chaiyen, P. (2010) A conserved active-site threonine is important for both sugar and flavin oxidations of pyranose 2-oxidase, *J. Biol. Chem. 285*, 9697–9705.
(39) Forneris, F., Heuts, D. P. H. M., Delvecchio, M., Rovida, S., Fraaije, M. W., and Mattevi, A. (2008) Structural analysis of the catalytic mechanism and stereoselectivity in *Streptomyces coelicolor* alditol oxidase, *Biochemistry 47*, 978–985.
(40) Yuan, H., and Gadda, G. (2011) Importance of a serine proximal to the C(4a) and N(5) flavin atoms for hydride transfer in choline oxidase, *Biochemistry 50*, 770–779.
(41) Yang, K.-Y., and Swenson, R. P. (2007) Modulation of the redox properties of the flavin cofactor through hydrogen-bonding interactions with the N (5) atom: role of αSer254 in the electron-transfer flavoprotein from the methylotrophic bacterium W3A1, *Biochemistry 46*, 2289–2297.
(42) Brondani, P. B., Dudek, H. M., Martinoli, C., Mattevi, A., and Fraaije, M. W. (2014) Finding the switch: turning a baeyer-villiger monooxygenase into a NADPH oxidase, *J Am Chem Soc 136*, 16966–16969.
(43) Mirza, I. A., Yachnin, B. J., Wang, S., Grosse, S., Bergeron, H., Imura, A., Iwaki, H., Hasegawa, Y., Lau, P. C. K., and Berghuis, A. M. (2009) Crystal structures of cyclohexanone monooxygenase reveal complex domain movements and a sliding cofactor, *J Am Chem Soc 131*, 8848–8854.
(44) Pazmiño, D. E. T., Snajdrova, R., Rial, D. V., Mihovilovic, M. D., and Fraaije, M. W. (2007) Altering the substrate specificity and enantioselectivity of phenylacetone monooxygenase by structure - inspired enzyme redesign, *Adv Synth Catal 349*, 1361–1368.
(45) Sheng, D., Ballou, D. P., and Massey, V. ( 2001) Mechanistic studies of cyclohexanone monooxygenase: chemical properties of intermediates involved in catalysis *Biochemistry 40*, 11156–11167.